LEVEL II ⑫

Project Report

SBR-2

D. M. Towle

DTIC
SELECTED
JAN 23 1981
E

Trapped Radiation Effects on the Space-Based Radar

14 October 1980

Lincoln Laboratory

MASSACHUSETTS INSTITUTE OF TECHNOLOGY

LEXINGTON, MASSACHUSETTS

81 1   23 003

This technical report has been reviewed and is approved for publication.

FOR THE COMMANDER

Joseph C. Syiek

Joseph C. Syiek
Project Officer
Lincoln Laboratory Project Office

MASSACHUSETTS INSTITUTE OF TECHNOLOGY

LINCOLN LABORATORY

TRAPPED RADIATION EFFECTS ON THE SPACE-BASED RADAR

D. M. TOWLE

Group 37

PROJECT REPORT SBR-2

14 OCTOBER 1980

LEXINGTON   MASSACHUSETTS

ABTRACT

This report presents the results of a parametric study regarding the influence of radiation damage effects on possible configurations of a phased array Space-Based Radar System. Primary emphasis is on Van Allen type trapped radiation effects on solar cells and on the antenna transmitter/receiver modules. Qualitative references to man-made nuclear radiation effects are also given. It is concluded that weight penalties for shielding against trapped radiation effects are sufficiently high in the intermediate altitude regime, 2,000 to 9,000 km altitude, to drive the design choices to higher or to lower altitude regimes.

Accession For

NTIS GRA&I ☒

DTIC TAB ☐

Unannounced ☐

Justification

By

Distribution/

Availability Codes

Avail and/or

Dist   Special

A

iii

TABLE OF CONTENTS

LIST OF ILLUSTRATIONS

1. INTRODUCTION

Due to a combination of circumstances, trapped radiation has greater significance for the Space Based Radar (SBR) than for most other satellite systems. Since the SBR concept utilizes a large phased array antenna,[1] the numerous antenna modules which are distributed throughout the antenna present, collectively, an exceptionally large surface area of vulnerable semiconductor devices. A large solar power supply will probably be utilized by the SBR also, and it too involves a large surface area of similarly vulnerable solid state solar cells. Restrictions on the shuttle payload weight allow only a relatively thin protective shielding to cover these large vulnerable areas. Additionally, the most desirable satellite orbits, from a systems point of view, are at intermediate altitudes where the trapped radiation environment is much harsher than for the geosynchronous or the low altitude orbits utilized by most other satellites.

This report presents the results of a series of calculations designed to predict the effects of space radiation on the SBR semiconductor devices in a variety of system configurations. The primary effects are due to the deterministically modelled trapped electron and proton radiation environment. However, the relatively minor effects of the stochastically modelled solar storms are also included in these calculations. As described in Section 4, semiconductor devices are the SBR components most vulnerable to trapped radiation effects. Previewing the conclusions; for intermediate altitude orbits between 1500 and 25,000 km it was found that advances in device hardness substantially beyond the present state-of-the-art will be required if a SBR satellite with adequate shielding is to be designed within the payload constraints of a single shuttle. For low altitude orbits (i.e., altitudes $\leq$ 1000 km) or for geosynchronous orbits the percentage weight penalty for shielding is not large enough to constitute a major feasibility problem.

1

The remainder of this report is organized as follows: Section 2 describes some of the SBR characteristics that are related to radiation vulnerabilities, Section 3 describes the radiation models, Section 4 discusses damage mechanisms, Section 5 presents the computational results, and Section 6 gives a discussion of results and the conclusions.

2

2. SYSTEM CONSIDERATIONS

The purpose of the SBR system is to provide timely surveillance of a variety of potential threats against the United States. The threat scenario definition and the SBR system configuration requirements are still undergoing evolution.[1] As an example of a likely goal, the SBR system could be designed to detect and to track hostile bombers traversing surveillance regions or fences around the Continental United States (CONUS). Numerous tradeoffs between the radar's size and its observational altitude are possible. Consideration has been given primarily to circular orbits in the low altitude (~1000 km), intermediate altitude (~10,000 km) and geosynchronous altitude (~36,000 km) categories. In general, the number of satellites required decreases and the power aperture of the individual radars increases as the SBR orbit altitude increases. System design and logistical practicalities tend to indicate that an intermediate altitude polar orbit would offer the most desirable balance between radar size and the number of satellites required.

A baseline system is defined here to provide a basis for specific examples of the significance of the calculated radiation effects on the SBR. Pertinent, approximate, parameters appropriate to an intermediate altitude system[2] are shown in Table 1.

TABLE 1
SBR BASELINE SYSTEM

Orbit	10,000 km altitude, circular polar
Antenna Diameter	50 m
Prime Power	25 Kw
Frequency	S-Band
Number of Antenna Modules	5×10^5

The parameter of greatest interest in regard to the objectives of this report is the total amount of surface area of the semiconductor devices. The distributed nature of the antenna array modules and the solar array cells result in a large area requiring distributed shielding. On the other hand, the electronics in the central processor for example, can be concentrated in a single compact box whose shielding weight requirements even with generous wall thickness are neglible compared to those of the distributed components.

One of the goals of the antenna module development program is to reduce the surface area of the S-band modules to about 4 cm^2 per side. Thus, the total surface area of all the modules in this baseline system amounts to about 400 m^2.

The total vulnerable surface area for the solar power supply can be estimated straightforwardly from the prime power requirements, the projected efficiency of the individual solar cells, and the solar constant. Assuming, somewhat optimistically, that solar cell efficiency of 20% will be achieved, the total surface area (both sides) of the solar array with 25 Kw capacity will be roughly 200 m^2. (A possible alternative to the solar power supply is a nuclear power supply which would have negligible vulnerable surface area. Its developmental status is less certain than the solar power supply. Additionally, a nuclear power supply would add its self-generated neutron radiation to the natural environment. The effect of such neutron radiation while probably negligible compared to the trapped radiation has not yet been evaluated. In this report, a solar power source is assumed.)

In regard to possible variations in the design from the baseline system as defined in Table 1, transmitter frequencies from L-band to X-band are still under consideration. Similar levels of radar performance at other radar frequencies[2] can be

4

obtained by adjusting the number of antenna modules in proportion
to the radar frequency. The total exposed area of the antenna
modules is thus roughly independent of the radar frequency since
the surface area of the individual modules tends to scale
approximately as the RF wavelength.

For low altitude orbits, an antenna diameter approximately
50% smaller than the intermediate altitude baseline system is
appropriate. For a geosynchronous system, an antenna diameter
at least 50% greater than the baseline system would be required.
The vulnerable antenna module area to be shielded, at a given
altitude, scales in proportion to the antenna area.

3. SBR RADIATION ENVIRONMENT

There are two separate types of ionizing radiation of primary concern for the SBR, namely, natural exoatmospheric radiation and man-made nuclear radiation. The natural radiation, although relatively weak and only slowly destructive, is probably of first concern because of its continual presence in the SBR domain. Man-made nuclear radiation, on the other hand, can cause very rapid deterioration of the SBR components. Nevertheless, a nuclear environment is likely to negate the SBR mission only under a limited set of credible scenarios as discussed below.

3.1 Natural Radiation

The natural radiation environment[3] of concern to the SBR is dominated by trapped electrons and protons in the Van Allen zones. It also includes solar photons, and in the outer regions, a less dense, but appreciable, free-flowing plasma composed mainly of protons of solar origin. A sketch depicting the occurrence of the various elements of the radiation environment which potentially are of concern to the SBR is shown in Fig. 1. The solar wind plasma flows against and around the earth's magnetic field. The outer reaches of the geomagnetic field lines, outside the trapped radiation zones of interest in Fig. 1, are distorted and pushed downstream by the flow of the solar plasma. The geomagnetic field shields the mid-to-low latitude regions of the exosphere out to about six earth radii against the direct free-flowing solar wind protons. It also holds the stable populations of secondary protons and electrons trapped in two diffusively defined belts inside this region. Individual charged trapped particles spiral along a given field line until reflected by the increasing gradient of field strength. In addition, the electrons drift gradually to the east and the protons to the west.
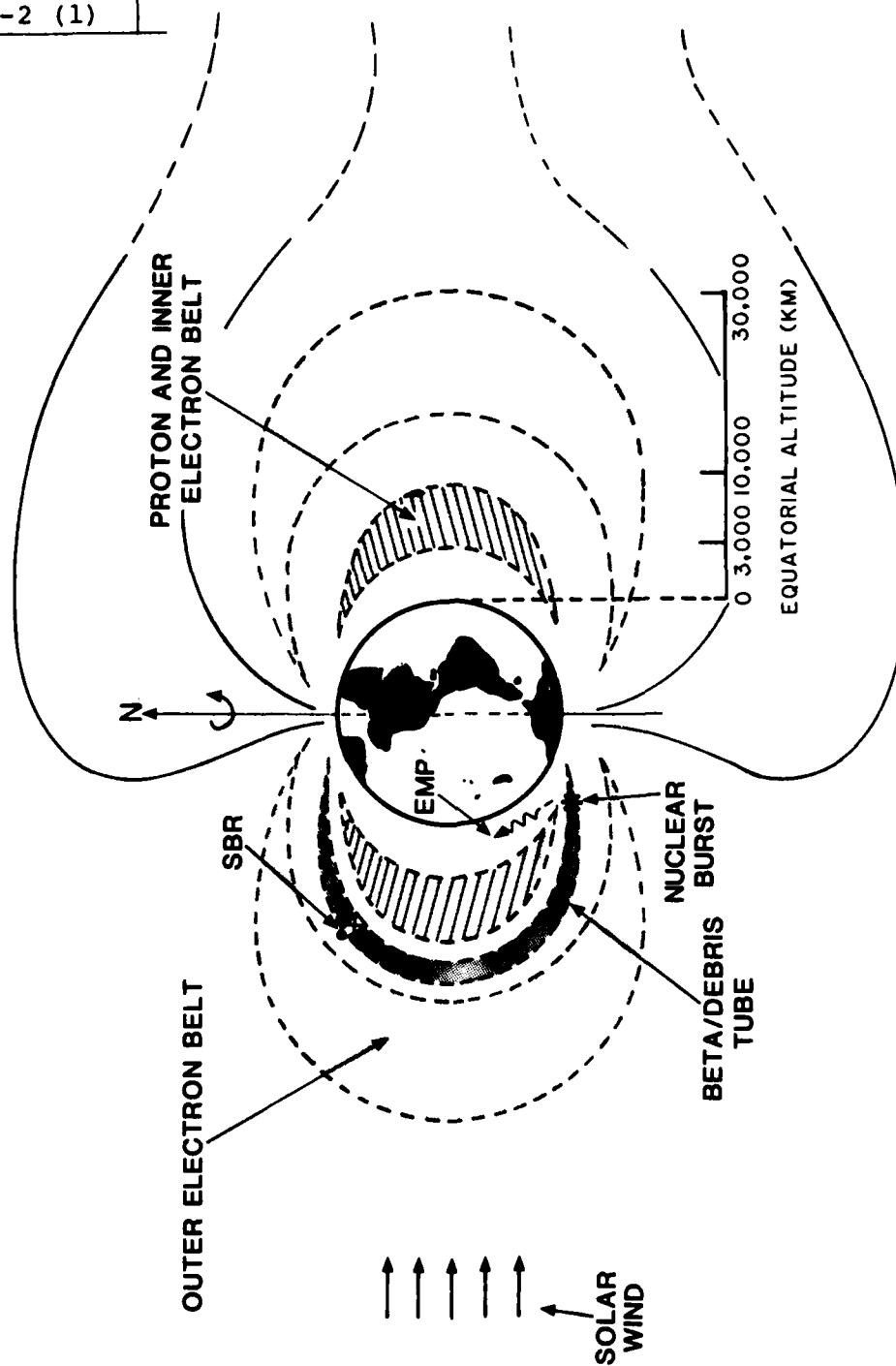
6

Fig. 1. Trapped radiation environment of the SBR system.

PROTON AND INNER ELECTRON BELT

EQUATORIAL ALTITUDE (KM)

0 3,000 10,000 30,000

N

EMP

SBR

NUCLEAR BURST

BETA/DEBRIS TUBE

OUTER ELECTRON BELT

SOLAR WIND

7

The most intense natural trapped radiation occurs in the inner Van Allen belt and consists of energetic protons and electrons, peaking at a L-shell* of about 1.4 corresponding to an altitude of 2500 km at the equator. A broad spectrum of particle energies occurs in this region with proton energies as shown in Fig. 2 exceeding 500 MEV and electron energies exceeding 5 MEV. The trapped particle population in the inner zone is generated by a complex interchange of cosmic and solar particles with the atmospheric particles which is not yet well understood.

Intense natural trapped electron radiation also occurs in the outer Van Allen zone and is generated by the solar wind. Although a trapped proton population exists in this region, without distinct geometric boundaries from the inner proton zone, its spectrum is much softer than in the inner zone. The trapped electron spectrum as indicated in Fig. 3 is quite broad, exceeding 5 MEV. The trapped radiation intensity of the outer zone peaks at a L-shell of approximately 3.5 corresponding to an equatorial altitude of 22,000 km.

During major solar proton events the rate of radiation dosage in regions not shielded by the geomagnetic field can increase for a few days by two orders of magnitude beyond the normal rate. Since only one or two major events are likely during the SBR 5-year lifetime, the cumulative dosage is expected to be small (≤ 10%), compared to the trapped radiation dosage in the midst of the Van Allen zones. Minor proton events occur on the order of once a month during the active half of the solar cycle but their cumulative dose over 5 years is generally less than for a single major event. The expected cumulative dosage from major and minor solar events is included in the simulation results described in Section 5, but its influence on the SBR is found to be small compared with trapped radiation effects.

---

*The L-shell number of a given field line is defined to be equal to the distance of the field line at the equator from the center of the earth, in units of the earth's radius.
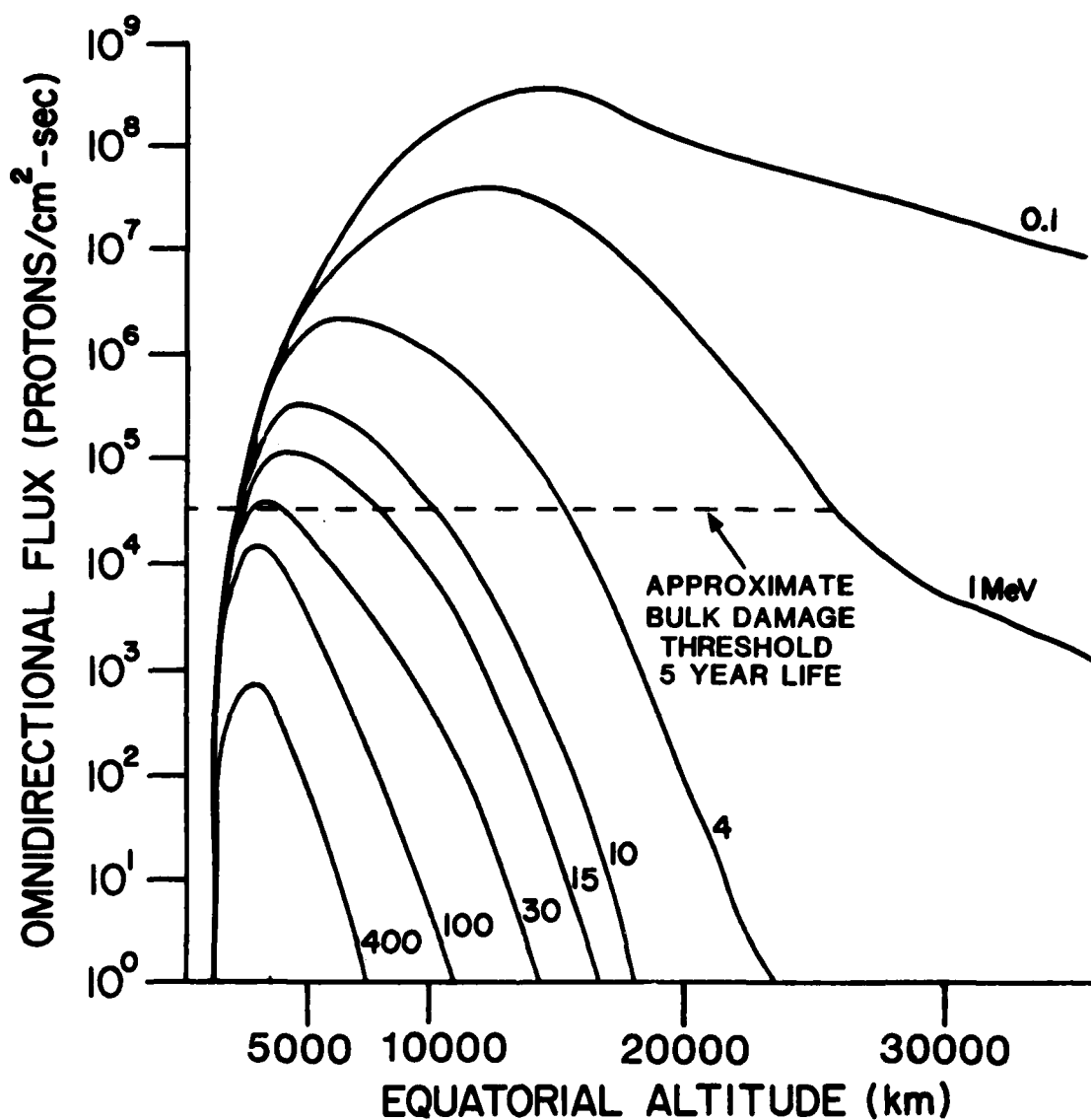
8

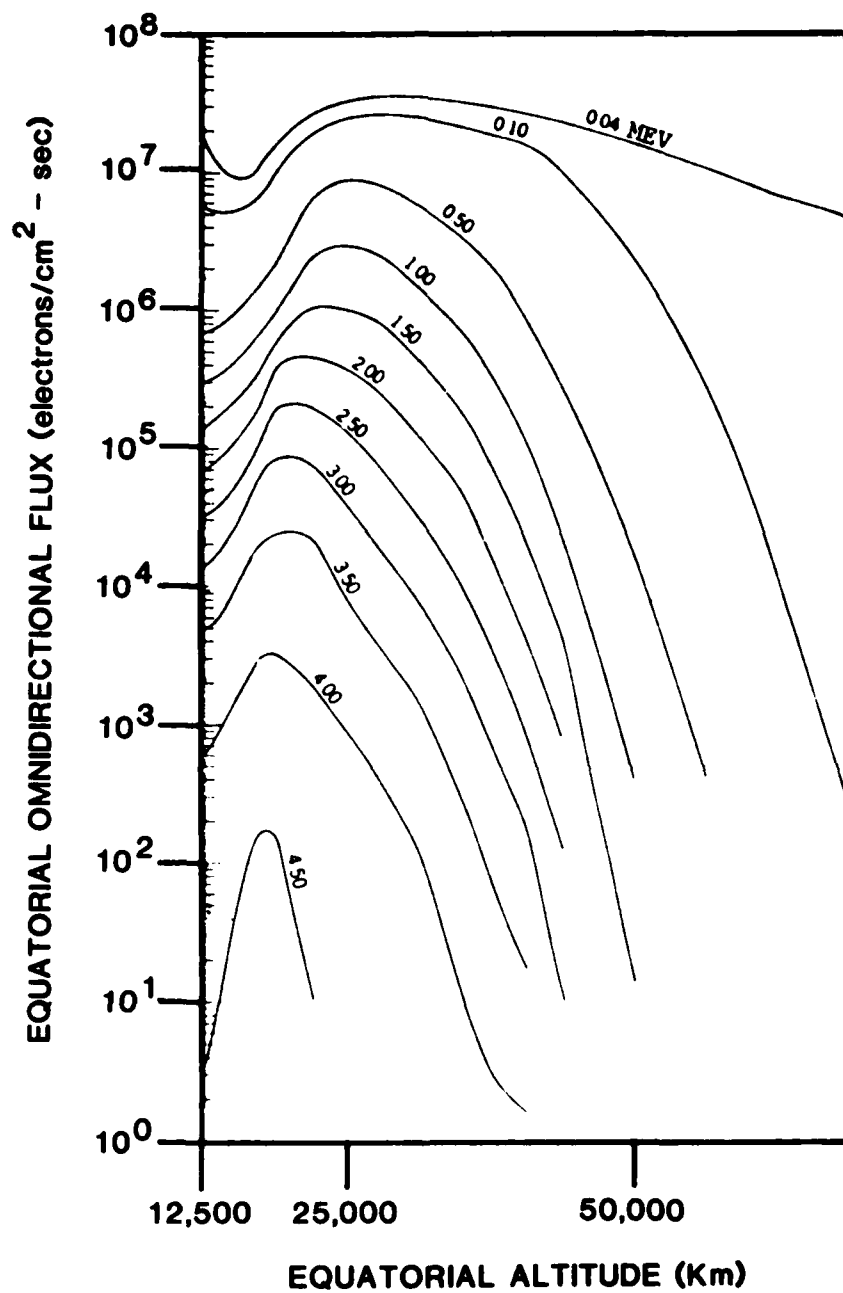Fig. 2. Equatorial omnidirectional proton flux distribution (AP8 MIN model).

Fig. 3. Outer belt electron flux (AE4 model).

10

3.2 Trapped Nuclear Radiation

An exoatmospheric nuclear burst produces numerous ions and free electrons which spiral along the geomagnetic field lines, initially forming a debris and a beta tube. Subsequently, in a matter of hours, these charged particles drift around the world forming an artificial trapped radiation belt with particle fluxes which may be substantially greater than in the natural belts. Except for the higher flux levels and a more penetrating trapped electron spectrum, the artificial radiation belts are quite similar to the natural trapped radiation belt. The higher flux levels and the harder spectrum makes satellite shielding more difficult however.

Most of the data on artificial trapped radiation belts were derived from U.S. and Russian exoatmospheric nuclear tests[3], in 1962, particularly the U.S. Starfish event. The Starfish burst (1 MT at 400 km altitude, latitude 15° N, L = 1.07) increased the dosage in the inner Van Allen zone sufficiently to cause serious damage to several lightly shielded satellites within a few days. The Starfish belt generated in July 1962, decayed slowly, reaching background levels only after several years. Some of the other exoatmospheric bursts at higher latitudes on higher L-shells formed artificial radiation belts which decayed within in few weeks.[3]

If multiple exoatmospheric bursts occur, the total flux generated in the artificial belt accumulates up to a predetermined saturation limit. An absolute upper limit is imposed by the fact that the geomagnetic field cannot contain particle flux if its kinetic energy density exceeds the potential energy of the field, i.e., $n_i M_i V^2/2 \leq B^2/8\pi$. (Particle density = n_i, particle mass = M_i, rms velocity = V, magnetic field strength = B.) The total potential energy of the geomagnetic field in the region encompassing the inner natural electron belt volumn is approximately

equal to the total kinetic energy of the electrons from approximately 100 MT of nuclear fission. Because Rayleigh-Taylor instabilities are likely to develop during the plasma expansions, the practical saturation load of the geomagnetic field is likely to be appreciably less than the absolute limit. Assuming that the inner zone can accumulate the equivalent of 10 Starfish bursts (i.e., 10% of the static limit which could be achieved by the detonation of 10 to 12 MT on L-shells 1.05 to 1.5) the dose rate in the inner zone would be up to three orders of magnitude greater than from the natural trapped radiation for many weeks after the bursts. Non-cooperative third country peacetime testing could produce this condition in a credible scenario. Precursor bursts at the start of a general warfare situation could also produce this condition but this scenario is of less concern since immediate kill of the satellites would not be likely and the SBR system could complete its major mission before failing.

Because the geomagnetic field strength is weaker at the higher L-shell numbers, an outer artificial belt generated by higher altitude and higher L-shell nuclear bursts would be expected to be much weaker and more rapidly dissipated than an inner artificial radiation belt.

Nuclear bursts also generate intense non-trapped radiation such as X-rays, gamma rays, and neutrons which are not treated explicitly in this report. Exoatmospheric kill radii for lightly shielded satellites of the order of 300 km for X-rays and 10 km for neutrons from moderate yield bursts would be anticipated. Even without detailed analysis it is obvious that the SBR cannot be effectively shielded against a direct attack. However, a direct attack would require synchronized strikes against the numerous SBR's and decoys all around the world and would constitute an unambiguous early warning. This type of scenario thus appears much less credible than one involving an artificial trapped

12

radiation belt formed by a few exoatmospheric bursts during peacetime tests by a third nation or by coincidental exoatmospheric bursts during a general warfare situation.

3.3 Computational Models

During the past several years, numerous measurements of trapped particle fluxes by use of satellite borne probes have been sponsored by NASA. NASA has also sponsored the development of semi-empirical computerized models based on these data which provide efficient calculation of the average flux levels to be anticipated. In the models, the flux levels are specified as functions of position in the geomagnetic field and the phase of the solar cycle. Current models of the natural particle environment and the integrated effects were obtained from NASA to perform the quanitative calculations of this report. The trapped proton models utilized were AP8MAC and AP8MIC, compact versions of AP8MAX and AP8MIN, respectively.[4] Non-trapped solar proton calculations utilized SOLPRO.[5] The trapped electron models were AE5MIN,[6] AE6MAX,[7] AEI8HI, and AEI7LO.[8] The NASA orbital flux integration program designated SOFIP[9] (Short Orbital Flux Integration Program) was used to calculate the accumulated fluence. For the results reported here a solar maximum period was used. The environmental models are for the most part representative of long term averages of the most credible data available from various space probes (AEI7HI which represents upper limit situations from a more limited set of data was not utilized in the reported results.) These models do not reflect local variations in the environment which are sometimes substantial but since the cumulative damage to the semiconductors depends on the integrated flux, and not on the fluctuations, this limitation is probably of little consequence.

An accurate Keplerian orbit calculation, typically at two minute intervals, was used to determine the path of the satellite through the trapped radiation belts. Flux integration was carried out over several integral orbits and then extrapolated to the 5 year SBR mission interval.

The detailed particle penetration and deposition calculations were carried out by use of "UNIDOSE" originated at RCA.[10] This program incorporates multiple infinite slab geometry and performs an analytic approximation to Monte Carlo scattering and deposition.

14

4.   DAMAGE MICROMECHANISMS

There are two major types of steady state radiation damage
to semiconductors; bulk damage involving crystalline atom dis-
placements and ionization damage involving charge buildup and/or
leakage currents. As a general rule, minority carrier devices
such as solar cells, diodes, and bipolar transistors are primarily
affected by bulk damage while majority carriers such as field
effect transistors (FET's) are usually most affected by ionization
damage. A sketch of the microprocesses involved in each type of
damage is shown in Fig. 4.

4.1 Bulk Damage

Referring to Fig. 4a, in regard to the microprocesses of
bulk damage, if a particle incident on a semiconductor crystal
collides with an atom (e.g., silicon) in the crystalline lattice
structure, it will displace the atom creating an interstitial
defect if it transfers approximately 10 ev of energy during the
collision. Protons are more effective at this displacement
process than electrons because of their greater mass and cross
section. An interstitial defect after formation acts as a
recombination center for the minority carriers, shortening their
mean diffusion path and thus reducing the output current and
decreasing the gain of the device. If the number of defects
becomes comparable with the minority carriers, then the device
ceases to operate properly.

4.2 Ionization Damage

Referring to Fig. 4b, in regard to ionization damage of
majority carrier devices, particularly insulated gate FET's,
incident particles or photons can ionize atoms along their paths
by transferring 4 ev or more to the valence electrons. (Lattice
displacements which may also occur are generally less injurious
to the operation of the device in the majority carrier case due
to the greater numbers of carriers.

MECHANISM	SEMICONDUCTOR TYPE
BULK DAMAGE (CRYSTALLINE DISPLACEMENTS)	MINORITY CARRIERS (SOLAR CELLS, DIODES, BIPOLAR TRANSISTORS)

BULK DAMAGE

DONOR →

MINORITY CARRIERS →

SEMICONDUCTOR CRYSTAL

PROTONS NEUTRONS (RADIATION)

DISPLACED ATOM (I2 EV)
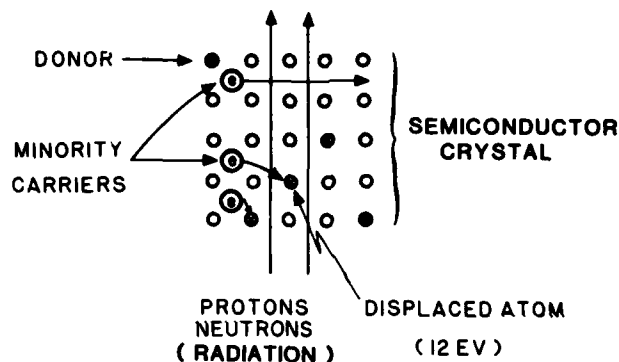
RADIATION	EFFECTS
PROTONS ELECTRONS NEUTRONS (NUC)	CRYSTAL DEFECTS FROM COLLISIONS MINORITY CARRIER LOSS TO DEFECTS SHORTER DIFFUSION LENGTH DECREASED COLLECTOR CURRENT, GAIN

Fig. 4(a). Principal semiconductor vulnerabilities.

16

MECHANISM   SEMICONDUCTOR TYPE

IONIZATION   MAJORITY CARRIERS

(FIELD EFFECT DEVICES, SOS)

IONIZATION DAMAGE

SUBSTRATE

MAJORITY CARRIERS

TRAPPED CHARGE

(4 EV)

BASE

PROTONS, γ RAYS, ELECTRONS
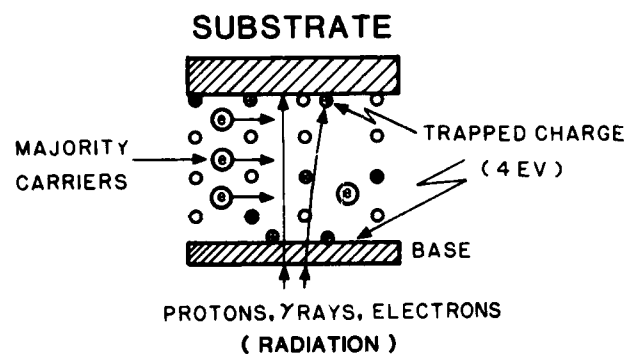
(RADIATION)

RADIATION   EFFECTS

PROTONS, ELECTRONS,   CRYSTAL DEFECTS LESS OF A PROBLEM

γ RAYS (NUC), X-RAYS   IONIZATION AT DIELECTRIC SUBSTRATE REBIASES TRANSISTOR

Fig. 4(b). Principal semiconductor vulnerabilities.

17

Experimental measurements of radiation effects on GaAs[11]
MESFETS, however, indicate that they are more sensitive to bulk
damage than to ionization damage.) When the ionization occurs at
a dielectric interface, the electrons tends to diffuse away but
the less mobile ions remain and accumulate over periods of years
in many cases, creating a net positive charge. If this positive
potential occurs in the insulated gate or in the substrate at
the edge of the device channel it rebiases the device, tending
to turn p-channel devices off and n-channel devices towards
saturation. Ionization of a surface with an applied bias also
causes an undesirable increase in leakage currents, sometimes
by an intolerable amount.

In addition to steady state damage effects, transient
radiation may cause serious circuit upsets if impulsive surface
ionization generates sufficiently high impulsive currents. The
dose rate from natural trapped radiation is not as a rule high
enough to cause this type of circuit problem. Transient ioniza-
tion by impulsive gamma radiation from nuclear bursts however may
cause circuit upset at long ranges from the burst. This problem,
which can be treated by the circuit designer without additional
shielding, is not addressed explicitly in this report.

Regardless of the complete details of the radiation damage,
the lifetime or durability of particular semiconductor devices
in a given environment can be predicted by making laboratory
measurements of the absorbed dose and the damage equivalent
normal incident fluence levels at which the devices fail.
Typically, for current state of the art devices, levels are 10^5
to 10^6 rad(Si) and 5×10^{14} to 5×10^{15} 1 Mev equivalent electrons
for majority and minority carrier devices, respectively.
Individual GaAs MESFET devices have been found[11] resistant to
ionization doses up to 10^8 rads(Si) and fluences up to 10^{15} 1 MEV
electrons. Techniques for fabricating VLSI GaAs MESFET devices
are currently beyond the state of the art, however.

4.3 Penetration and Deposition of Particle Radiation

The localization of radiation effects within a semiconductor device depends to a large extent on the energy of the incident radiation and on the amount of intervening material. Figure 5 indicates the thickness, or equivalently the linear mass, of aluminum which can be penetrated by protons as a function of the proton energy. A 10 Mev proton can penetrate about .18 gm/cm^2 or 25 mil of aluminum. Figure 5 also applies approximately to glass (or fused silica) since the density of glass and aluminum are similar and the particle penetration, in terms of linear mass penetrated is nearly independent of the material.

A sketch illustrating qualitatively the penetration and deposition characteristics of protons within several discrete energy bands incident on a semiconductor device covered by a 25 mil aluminum sheet is shown in Fig. 6. Protons with less than 1 Mev energy are absorbed essentially at the surface of the first material encountered. While protons with energies greater than about 100 Mev penetrate completely through the (25 mil) aluminum sheet leaving a nearly uniform but relatively sparse trail of ionization and dislocations in the semiconductor device. As indicated in Fig. 6, protons with intermediate energies just sufficient to penetrate to the critical regions of the device cause the majority of the damage. There are two basic reasons for this. First, for normal trapped particle distributions, there are more particles with intermediate energies than there are with high energies and secondly, the particle collisions tend to occur at much higher density near the end of their penetration path. Since there is a continuum of particle energies in the natural distributions (unlike the discrete bands illustrated in Fig. 6), there is always a band of energies appropriate for deposition in the vital region of the device, regardless of the thickness of the shield, unless
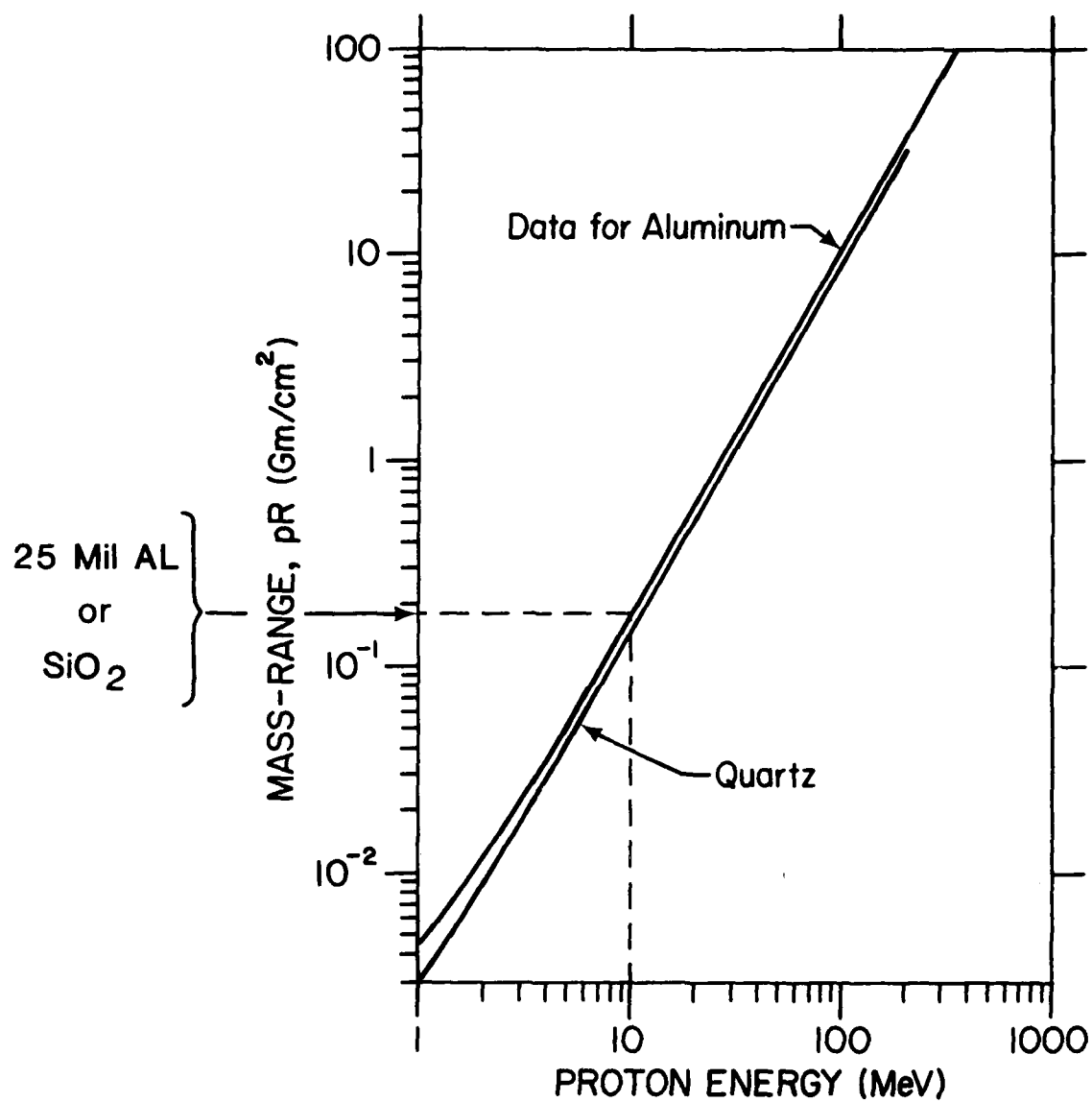
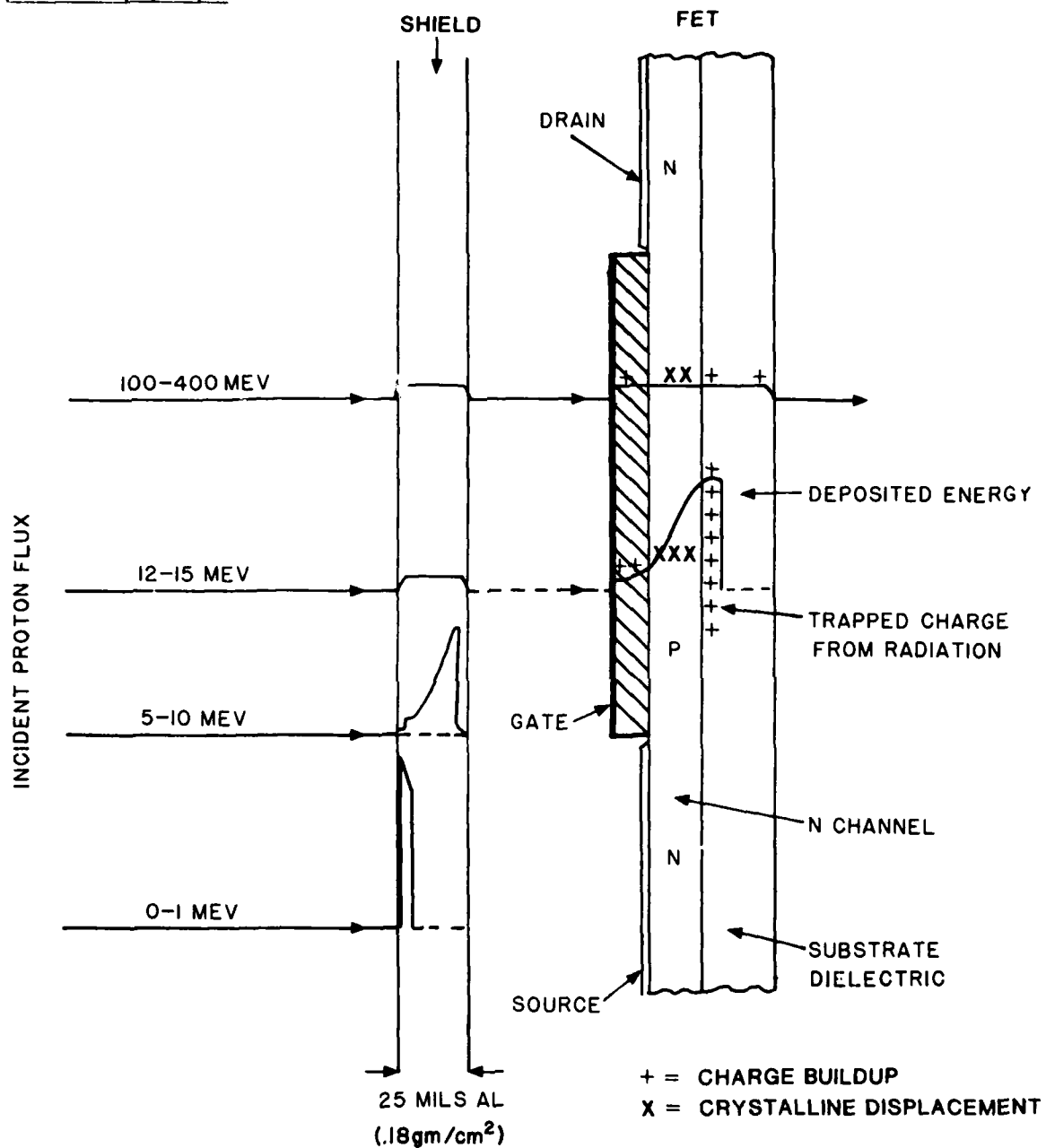Fig. 5. Mass-range for protons through aluminum and quartz.

Fig. 6. Radiation deposition and ionization in shield (25 mil Al)
and in insulated gate field effect transistor.

it is thick enough to stop all of the radiation. The absorbed internal dose decreases as the shield thickness increases for natural particle distribution because the flux decreases monotonically with energy. Similarly, since the trapped particles are isotropically distributed, most transit the shield at obtuse angles, thus experiencing effectively thicker shielding as the angle of incident becomes more acute and are filtered accordingly.

As a simple illustration of shielding effectiveness, con·ider the proton flux with the spectrum indicated in Fig. 2 incident on a 25 mil aluminum sheet. The lowest energy protons are all absorbed in the aluminum sheet. The magnitude of the emerging flux is greatly reduced and has a degraded spectrum as indicated in Fig. 7. The level of flux of the degraded spectrum which a typical semiconductor device could withstand over a 5 year period with gradual deterioration to an inoperative level is indicated roughly by the dashed lines in Figs. 2 and 7. As far as the proton radiation alone is concerned, this approximate analysis indicates that the 25 mil shield would be sufficient to protect the device in an equatorial orbit at altitudes less than 2000 km or greater than 10,000 km, but would be grossly inadequate in the intermediate altitude region.

More exact analysis needs to take into account the combined presence of the electrons and the protons, the quanitative equivalence of semiconductor damage at various particle energies for both species, detailed deposition of the particles, geometry effects, and precise orbital position and flux integration. This procedure has been carried out with the aid of the computerized models described briefly in the previous section and the results reported in the next section.
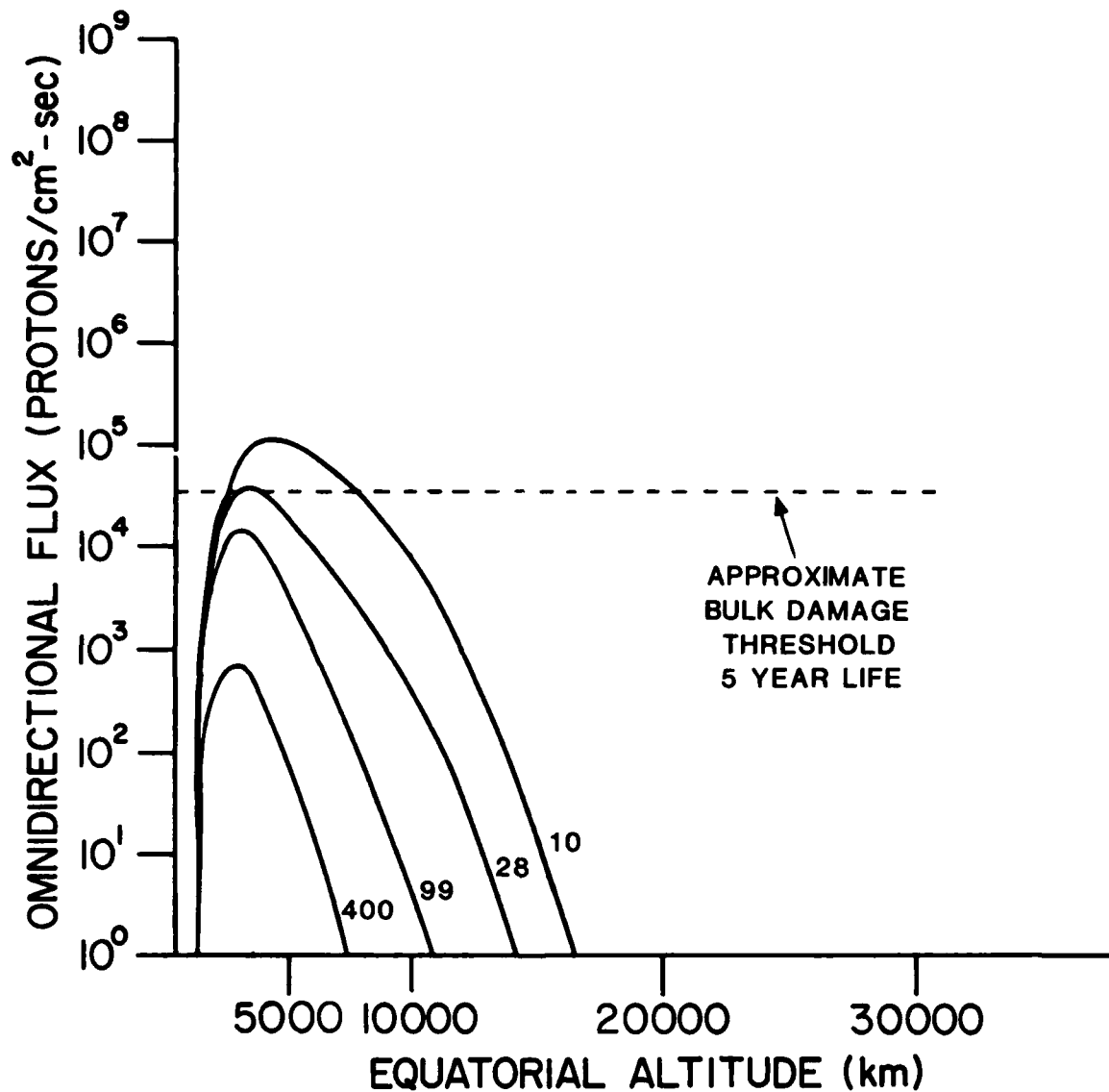
Fig. 7. Equatorial omnidirectional proton flux distribution through 25 mil Al shield (AP8 MIN model).

5. RESULTS

Because the natural trapped radiation environment is strongly
dependent on the satellite orbit, a parametric set of orbits was
selected for the computer simulations of the SBR exposure. Most
of the simulated orbits were circular with inclinations of
$0°$, $60°$, and $90°$ at altitudes between 1000 and 40,000 km. These
were selected to aid in the final choice of orbits. A Molniya
type orbit ($63°$ inclination, altitude 500 to 40,000 km) was also
simulated. In addition, damage thresholds were parameterized
to allow the assessment of the benefit of increasing the hardness
rating of the components.

Two different classes of damage effects were considered,
bulk (or displacement) damage generally appropriate for minority
carrier devices and ionization damage appropriate for many
majority carrier devices. Since both types of devices are likely
to be utilized, the final SBR design must make shielding pro-
visions for both types of semiconductor damage.

5.1 Bulk Damage

The radiation exposure of an orbiting satellite is generally
due to a mixture of incident particle fluxes. For comparison
purposes, an equivalent common measure of exposure is needed.
For the reslts reported here, the proton fluence was converted
to an equivalent 1 MEV electron fluence. To accomplish this,
the proton spectra were divided into 10 MEV bands which were then
multiplied by an equivalency factor of 790. This factor is
approximately appropriate for proton effects on most of the
minority carrier semiconductor devices. However, it underestimates
the proton effects on the solar cells in a solar power supply by
a factor of three thus their nominal damage thresholds as utilized
in this report have been adjusted downward accordingly.

24

The fluence resulting at various depths inside flat, one-dimensional aluminum or glass layers from the total fluence incident along the satellite orbit, extrapolated to 5 years exposure was calculated. By utilizing numerous parameterized layer depths, shield thickness were determined which would reduce the incident radiation to preselected threshold levels for a variety of orbits.

The plane geometry assumed in the shielding calculations, while not precise, is more nearly appropriate to the SBR component geometry than spherical geometry would be. Conversion to spherical or to compound geometries can be approximated readily from the plane geometry results, if needed.

The results of these simulations for bulk damage effects are shown in Figs. 8, 9, and 10 for orbits with inclinations of 0°, 60°, and 90°, respectively. The thickness of aluminum or glass covers which would be required to reduce the fluence incident on the satellite surface over 5 years to preselected levels ranging from easily tolerable to one or two orders of magnitude above tolerable for current minority carrier devices are plotted vs altitude. Shielding thickness requirements for bulk damage effects on the SBR in a Molniya type orbit are indicated by dashed lines in Fig. 9.

The failure of solar cells is not usually discontinuous. Typically, current device output would be reduced by 10% at the lowest threshold, 25% at the next and 50% at the highest fluence threshold utilized in this report.

The most energetic protons occurring in the lower portion of the inner belt are responsible for the high peak in shielding thickness requirements at altitudes around 3000 km, particularly for equatorial orbits. Satellites in highly inclined orbits at this altitude spend only a fraction of their time in the most intense region and thus are less affected than those in similar

Fig. 8. Shield thickness requirements for components subject
to bulk damage (equatorial orbits).

26

Fig. 9. Shield thickness requirements for components subject to bulk damage (inclined orbits).

INCLINED
CIRCULAR ORBITS
INCLINATION = 60°

HARDNESS THRESHOLDS
Th I = $10^{14}/cm^2$
Th II = $10^{15}/cm^2$
Th III = $10^{16}/cm^2$
1MEV EQUIVALENT
ELECTRONS, FLUENCE

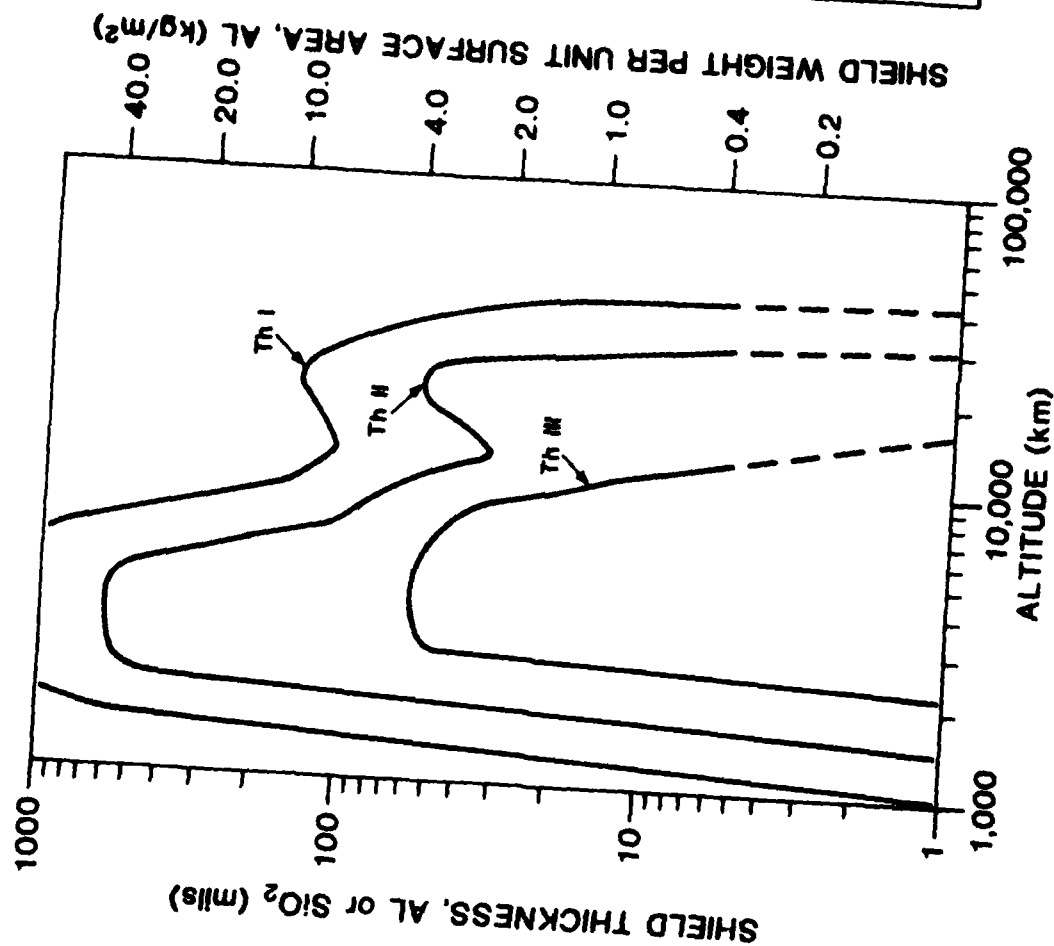SHIELD WEIGHT PER UNIT SURFACE AREA, AL (kg/m²)

SHIELD THICKNESS, AL or SiO₂ (mils)

ALTITUDE (km)

27

Fig. 10. Shield thickness requirements for components subject to bulk damage (polar orbits).

28

equatorial orbits. The energetic electrons in the outer-belt lead to a secondary peak at about 20,000 km altitude which is notable only for the lower threshold or thicker shield cases. The secondary peak due to the outer belt electrons is small in comparison to that in the inner zone, primarily because the electrons are less efficient in causing crystalline displacements than protons are. Thus minority carrier devices affected primarily by crystalline displacements, such as solar cells and bipolar transistors, are more severely affected by the proton belt than by either of the two electron belts.

5.2 Ionization Damage

In contrast to bulk damage processes, electrons are more effective than protons in causing ionization damage of particular concern to majority carrier devices. The shielding requirements to reduce ionization effects to tolerable levels are strongly influenced by the intensity of the trapped electrons in both the inner and the outer trapped electron zones. There simulation results for ionization damage are shown in Figs. 11, 12, and 13 for circular orbits with inclinations of 0°, 60°, and 90°, respectively. They are displayed in a form similar to the bulk damage results. The thickness of aluminum or glass covers required to reduce the incident dose down to preselected levels near and incrementally above anticipated tolerable levels for majority carrier devices is plotted vs satellite altitude.

Satellites in orbits with equatorial altitudes around 4000 km and 20,000 km require the most shielding to reduce ionization doses to tolerable levels. In between the inner and outer Van Allen zones, at about 10,000 km equatorial altitude appreciably less shielding is required than in the middle of either belt. For equatorial orbits, the locally reduced ionization dose region is narrow in altitude extending effectively between 9000 and 11,000 km. For polar orbits, the shielding
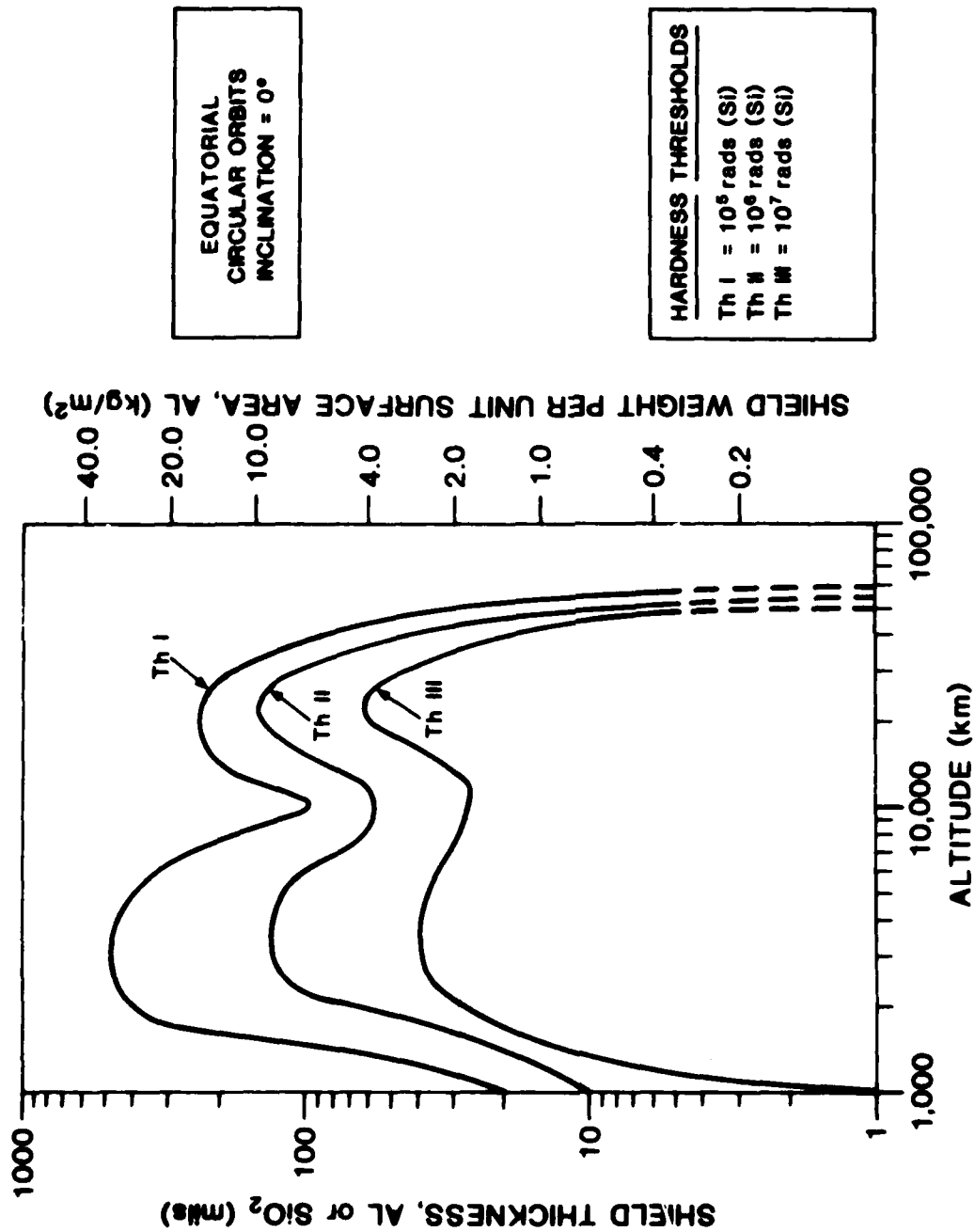
Fig. 11. Shield thickness requirements for components subject to ionization damage (equatorial orbits).
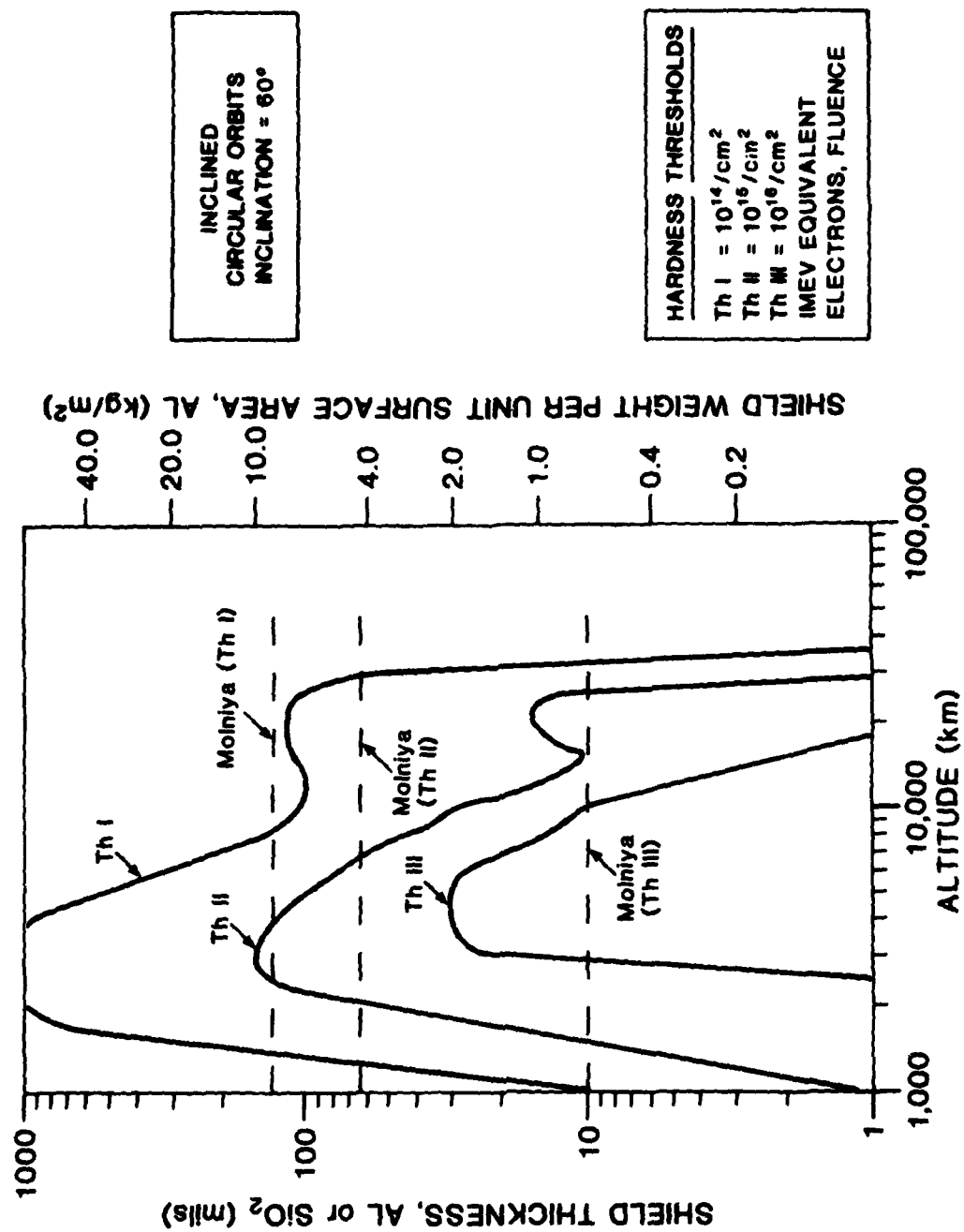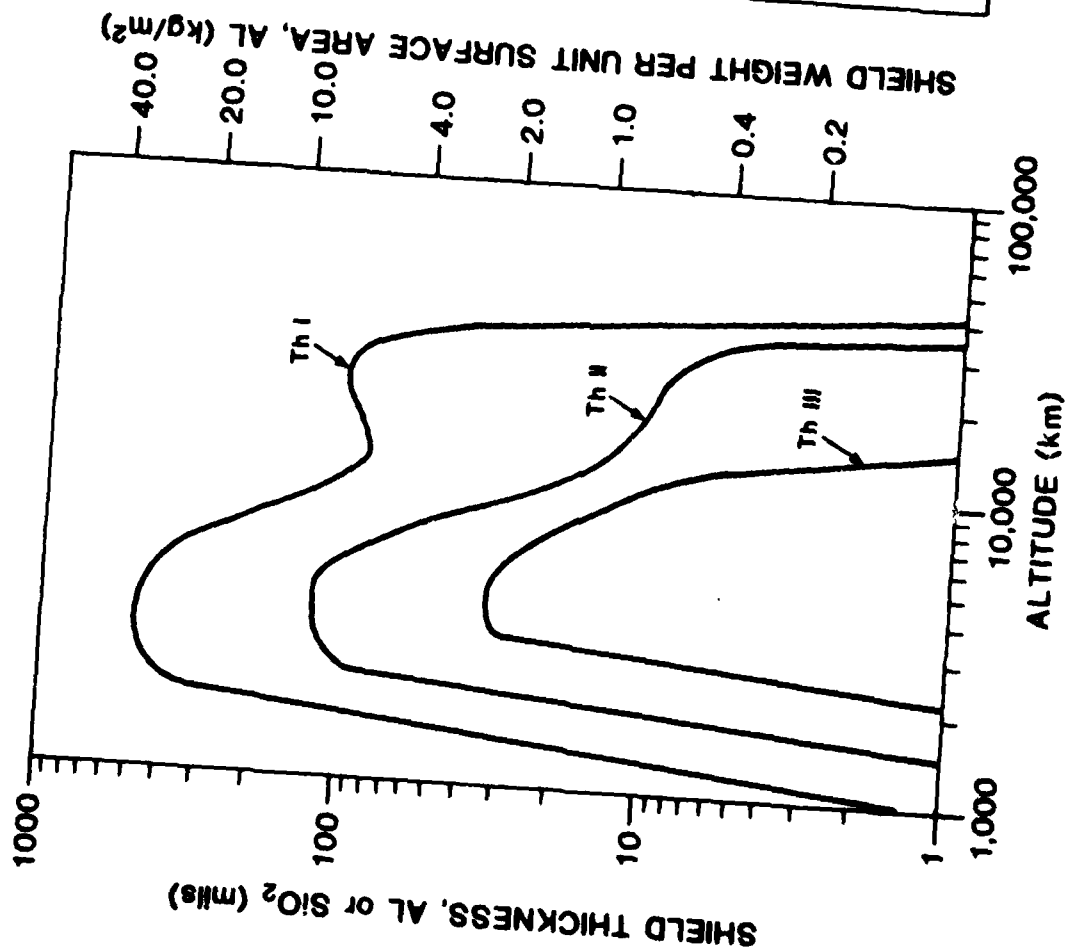
30
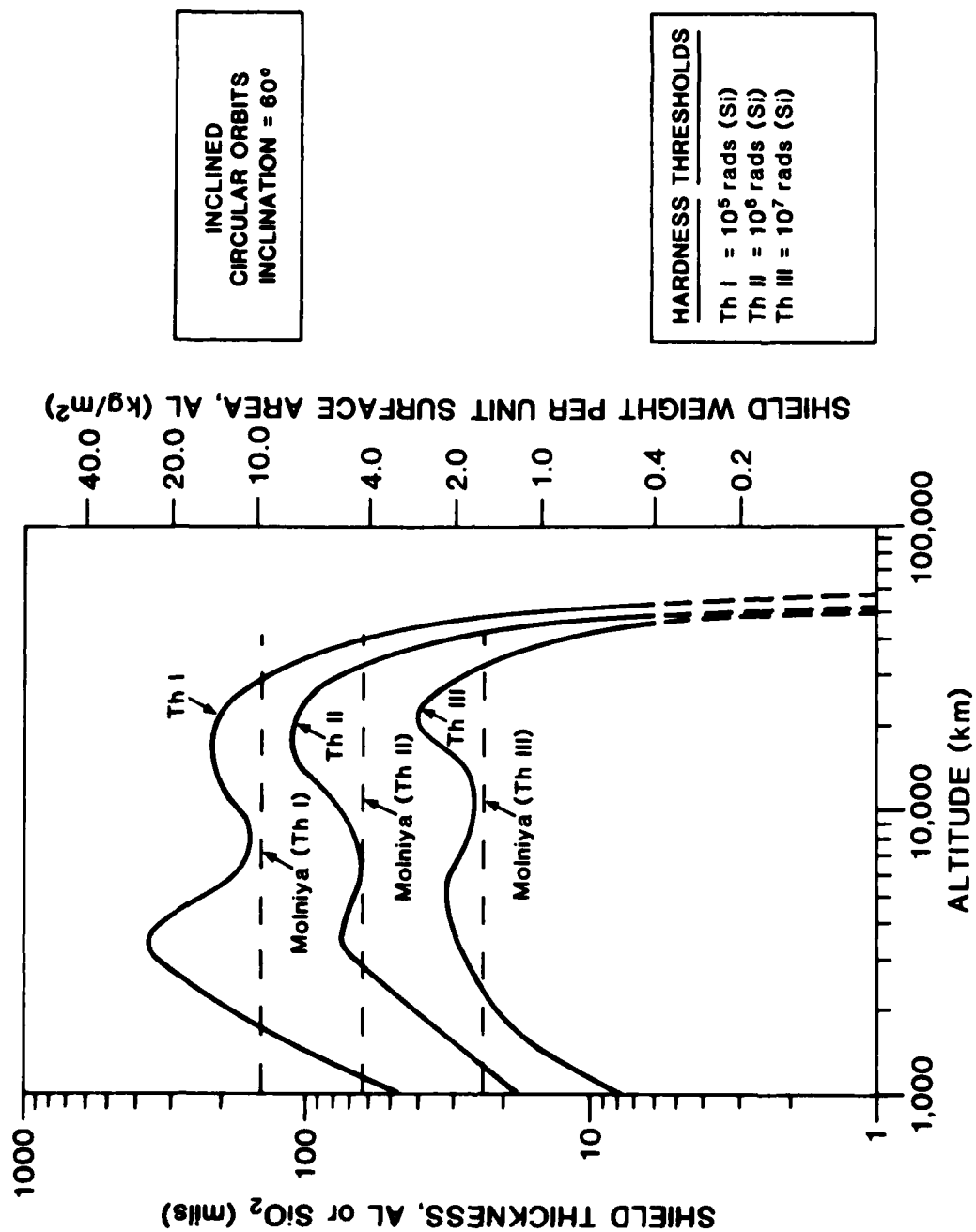
Fig. 12. Shield thickness requirements for components subject to ionization damage (inclined orbits).

31

POLAR
CIRCULAR ORBITS
INCLINATION = 90°

HARDNESS THRESHOLDS

Th I = 10^5 rads (Si)
Th II = 10^6 rads (Si)
Th III = 10^7 rads (Si)

SHIELD WEIGHT PER UNIT SURFACE AREA, AL (kg/m²)

40.0   20.0   10.0   4.0   2.0   1.0   0.4   0.2

100,000

Th I
Th II
Th III

ALTITUDE (km)

10,000

1,000

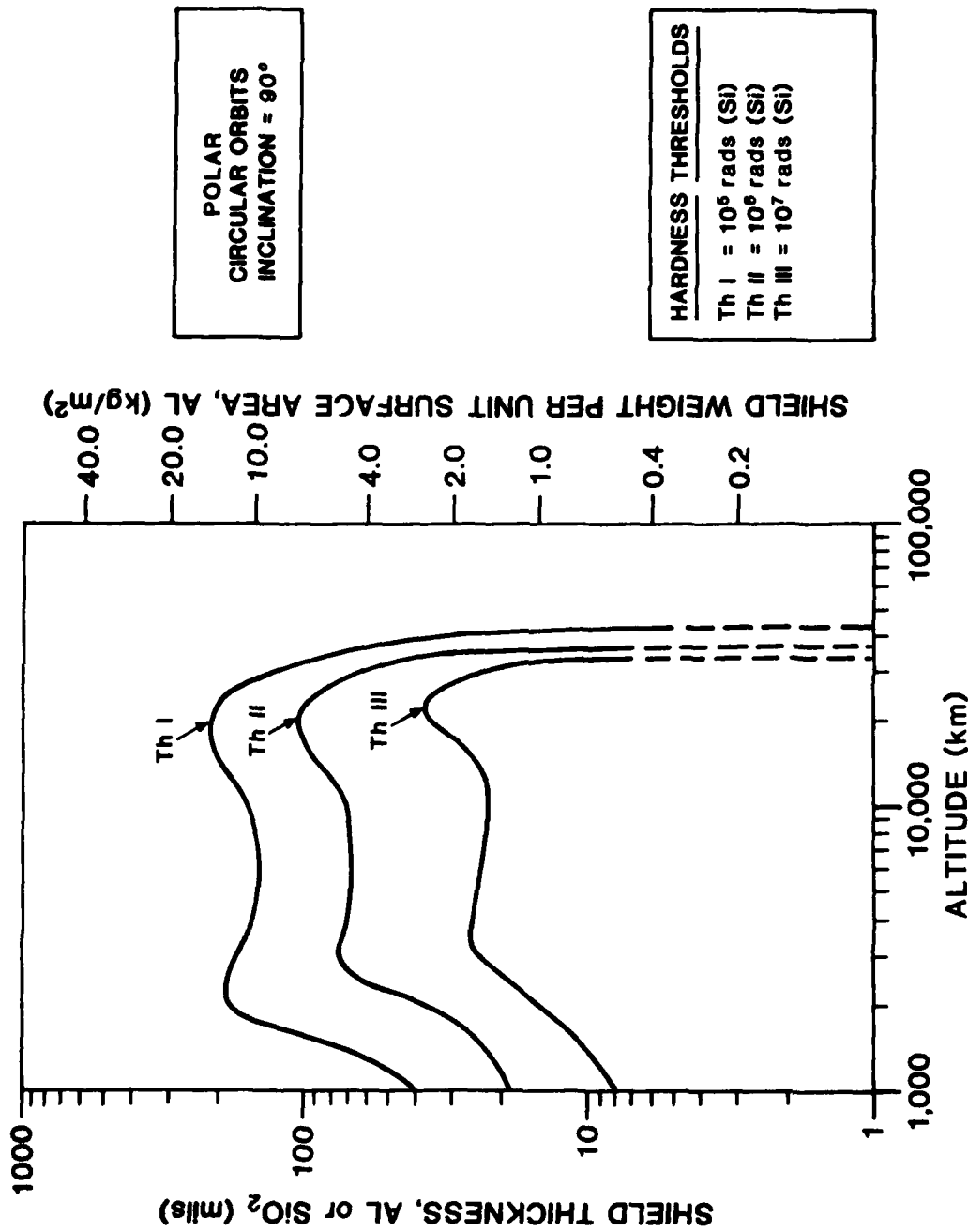1000

100

10

1

SHIELD THICKNESS, AL or SiO₂ (mils)

Fig. 13. Shield thickness requirements for components subject
to ionization damage (polar orbits).

32

requirements for ionization effects alone are nearly flat from 4000 to 11,000 km altitude with a peak at 20,000 km and a very sharp fall above 30,000 km. The very harsh bulk damage effects in the inner zone, shown in Figs. 8, 9, and 10, would tend to inhibit the use of orbits in the region between 2000 and 9000 km equatorial altitude regardless of this reduced ionization damage for polar orbits however.

In spite of the sizable dip in both types of exposure around 10,000 km equatorial altitude, the shielding requirements for the SBR in that region are considerably higher than for altitudes below 1500 km or above 30,000 km and would be difficult to meet unless a breakthrough in hardening technology occurs. As an example, for moderately optimistic thresholds (10^6 rad Si) for majority carrier devices and 10^{15} 1 MEV Equivalent Electron Fluence for solar cells) 400 kilograms of shield weight per 100 M^2 of antenna module surface area and 150 kilograms per 100 M^2 of solar cell area would be required for a 10,000 km altitude circular orbit. Optimistic estimates of surface area, 200 M^2 for solar cells and 400 M^2 for antenna models indicate that 1900 kgm of shielding would be required at this level of hardness. For current state of the art hardness levels (10^5 rads (Si) and 5×10^{14} MEV Equivalent Electron Fluence) a factor of 3 more, or 5700 kgm, of shielding would be required. With very optimistic advances in hardness levels (10^7 rad (Si) and 16^{16} 1 MEV Equivalent Electrons) a factor of 3 less or 600 kgm of shielding would be required. Only the latter figure is compatible with single shuttle payload limitations.

For a Molniya type orbit (500 km perigee, 30,000 km apogee, 63° inclination) the radiation exposure is very similar to a 10,000 km altitude circular polar orbit and equivalent amounts of shielding would be required as indicated by the dashed lines in Fig. 12.

5.3 Trapped Nuclear Radiation

Trapped nuclear radiation effects were not quantitatively
modeled for this report, but were estimated from existing materal.[3]
It is assumed from the considerations discussed in Subsection 3.2
that the most severe artificial radiation belt buildup realizable
is an order of magnitude greater than the Starfish belt and
could be generated by about 10 MT of fission yield from a few exo-
atmospheric bursts on low L-shells. The strongest artificial
belt would encompass a region approximately coincident with the
inner electron belt but extending down to somewhat lower altitudes
due to the higher energy fission electrons.

The incident flux from this artificial belt in the equatorial
altitude region of 1000 to 10,000 km would be nearly three orders
of magnitude higher than in the natural belt and have a harder
electron spectrum. A surface dose of 10^7 rads (Si) would accumu-
late in a single day in this region. Shielding would be more
difficult than in the natural radiation case due to the harder
electron spectrum which generates copious bremstrahlung. This
secondary radiation penetrates thick shields readily and ionizes
internally. As a consequence, the expected lifetime of an SBR
shielded appropriately for 5 year lifetime in the natural environ-
ment at 10,000 km would be of the order of a few days in this
environment. For polar orbits in the 500 to 1000 km altitude
region the lifetime of a lightly shielded SBR in the nuclear
environment would be of the order of a few weeks as compared to
an indefinitely long lifetime in the natural environment. For
geosynchronous altitudes or above, no appreciable nuclear trapping
is expected and consequently the influence of remote incidental
nuclear bursts on SBR's operating in that region would be
negligible.

6. DISCUSSION AND RECOMMENDATIONS

6.1 Natural Trapped Radiation Considerations

The results of the environmental effects analysis in the previous section show that the natural trapped radiation needs to be taken into account during the planning and the designing phases of the SBR system. If, as an extreme example, it were necessary to operate the SBR in orbits which intercept the most intense natural trapped radiation regions, i.e., circular orbits of approximately 3000 km altitude, the operational lifetime of the solar cells and the antenna modules would be reduced to a few months even if half the shuttle payload were devoted to shielding.

If, on the other hand, it were decided to utilize orbits, either above (e.g., 36,000 km altitude) or below (e.g., 1000 km altitude) the most intense natural radiation zones, adequate shielding for the system could be designed with shielding weight requirements (as indicated by Fig. 9 and 11) at only a small fraction of the total system weight. Whether such constraints unduly interfere with other system operational and logistics requirements is the subject of separate system studies.[1]

An assessment of the practicality of utilizing intermediate altitude, inclined circular, orbits of approximately 10,000 km altitude which would take advantage of a local minimum between the inner and outer radiation zones and which has some systems advantages requires more tentative conclusions. At the present time it appears that some technical breakthroughs will be required, if this type of orbit is to be utilized for an SBR satellite with lifetime requirements of the order of 5 years. First, note from Fig. 9 that a 25 kw solar power supply with at least 200 M^2 surface area in a 10,000 km altitude polar orbit would require at least 400 kgm of shielding for 5 years of lifetime. (Alternatively, a nuclear power supply of equivalent

35

capacity would have to be developed.) In addition, either the
inherent hardness of the antenna module electronics would have
to be improved considerably (to roughly 10^8 rads (Si) and 10^{16} 1
MEV Equivalent Electrons) or else the cumulative surface area of
the modules reduced by an order of magnitude (i.e., to 40 M^2
for both sides). The prospects of achieving an acceptable
combination of these developments during the next few years
appears uncertain. GaAs MESFETs show some promise for sufficient
ionization hardness but prospects for their fabrication into
acceptable VLSI modules are questionable. Silicon on sapphire
IGFET's would require at least two orders of magnitude improve-
ment in ionization hardness. Thus, the first generation of
SBR's at least, probably will be forced to utilize orbits
either above or below the worst of the natural radiation belts.

6.2 Nuclear Radiation Considerations

This report does not attempt to deal with the prompt kill
effects of the radiation (i.e., intense X-rays, gamma rays, and
neutrons) from nearby nuclear bursts explicity. It is conceded
that the SBR cannot be effectively shielded against a direct
one-on-one nuclear attack unless some highly successful keep-out
defense is invoked.

It is concluded, however, that an artificial nuclear trapped
radiation belt environment is credible and should be taken into
account during the system planning and design stage. In particular,
peacetime testing of several megatons by a non-cooperative country
could create an artificial trapped radiation belt which would reduce
the lifetime of a mid-altitude SBR to the order of a few days and
a low altitude SBR to the order of a few weeks. In such a
situation, a geosynchronous altitude orbit for the SBR would be
highly preferable since it would place the SBR outside most of
the radiation of an artificial trapped radiation belt.

A similar conclusion applies also to the situation involving an artificial nuclear radiation belt formed by multiple coincidental exoatomospheric bursts during the start of a general warfare situation. However, in that case the SBR could presumably perform its major function before succumbing (discounting the possibility of a successful direct attack on the SBR) even at intermediate altitudes. For this situation, in addition to trapped radiation effects, two other remote burst effects, namely, transient radiation effects and EMP effects should be taken into account during the SBR design. Techniques currently exist which can minimize these nuclear effects without adding severely to the total system weigth.

REFERENCES

{1} J. Schultz and P. Nosal, "Space-Based Radar," in Space World P-5-185 (May 1979), pp. 4-11.

{2} D. R. Olsen, private communication (July 1979).

{3} J. B. Cladis et al., "The Trapped Radiation Handbook," Defense Nuclear Agency, DNA 2524H (January 1977).

{4} D. M. Sawyer and J. I. Vette, "AP-8 Trapped Proton Environment for Solar Maximum and Solar Minimum," National Space Science Data Center, NSSDC 76-06 (December 1976).

{5} E. G. Stassinopoulis, "SOLPRO: A Computer Code to Calculate Probalistic Energetic Solar Proton Fluences," National Space Science Data Center, NSSDC 75-11 (April 1975).

{6} M. J. Teague and J. I. Vette, "A Model of the Trapped Electron Population for Solar Minimum," National Space Science Data Center, NSSDC 74-03 (April 1974).

{7} M. J. Teague, K. W. Chan, and J. I. Vette, "AE6: A Model Environment of Trapped Electrons for Solar Maximum," National Space Science Data Center, NSSDC 76-04 (May 1976).

{8} M. J. Teague and J. I. Vette, "AEI7Hi and AEI7Lo, Interim Outer Zone Trapped Electron Models," National Space Science Data Center (to be published).

{9} E. G. Stassinopoulis, et al., "SOFIP: A Short Orbital Fluz Integration Program," Goddard Space Flight Center, X-601-77-114 (May 1977).

{10} R. S. Ohanian, "UNIDOSE: A Computer Program to Calculate Energetic Particle Deposition," Astro-Electronics Division, RCA, private communication (July 1979).

{11} J. M. Borrego et at., "Radiation Effects on GaAs MESFETS," Proceedings IEEE Annual Nuclear and Space Radiations Effects Conference (IEEE, New York, December 1978), pp. 1436-1443.

GLOSSARY

CONUS	Continental United States
FET	Field Effect Transistor
IGFET	Insulated Gate Field Effect Transistor
MESFET	Metal Schottscky Field Effect Transistor
NASA	National Aeronautics and Space Administration
SBR	Space Based Radar
SOS	Silicon on Sapphire
VLSI	Very Large Scale Integrated

SECURITY CLASSIFICATION OF THIS PAGE (When Data Entered)

REPORT DOCUMENTATION PAGE	READ INSTRUCTIONS BEFORE COMPLETING FORM

1. REPORT NUMBER	2. GOVT ACCESSION NO.	3. RECIPIENT'S CATALOG NUMBER
ESD-TR-80-215	AD-A094065	

4. TITLE (and Subtitle)	5. TYPE OF REPORT & PERIOD COVERED
Trapped Radiation Effects on the Space-Based Radar	Project Report
	6. PERFORMING ORG. REPORT NUMBER
	Project Report SBR-2

7. AUTHOR(s)	8. CONTRACT OR GRANT NUMBER(s)
David M. Towle	F19628-80-C-0002
	ARPA Order-3724

9. PERFORMING ORGANIZATION NAME AND ADDRESS	10. PROGRAM ELEMENT, PROJECT, TASK AREA & WORK UNIT NUMBERS
Lincoln Laboratory, M.I.T. P.O. Box 73 Lexington, MA 02173	ARPA Order 3724 Program Element No. 62301E Project No. 1E20

11. CONTROLLING OFFICE NAME AND ADDRESS	12. REPORT DATE
Defense Advanced Research Projects Agency 1400 Wilson Boulevard Arlington, VA 22209	14 October 1980
	13. NUMBER OF PAGES
	46

14. MONITORING AGENCY NAME & ADDRESS (if different from Controlling Office)	15. SECURITY CLASS. (of this report)
Electronic Systems Division Hanscom AFB Bedford, MA 01731	Unclassified
	15a. DECLASSIFICATION DOWNGRADING SCHEDULE

16. DISTRIBUTION STATEMENT (of this Report)

Approved for public release; distribution unlimited.

17. DISTRIBUTION STATEMENT (of the abstract entered in Block 20, if different from Report)

18. SUPPLEMENTARY NOTES

None

19. KEY WORDS (Continue on reverse side if necessary and identify by block number)

space-based radar	solar power
radiation damage	nuclear radiation
parametric study	Van Allen radiation belt
phased array antenna	satellite orbits

20. ABSTRACT (Continue on reverse side if necessary and identify by block number)

This report presents the results of a parametric study regarding the influence of radiation damage effects on possible configurations of a phased array Space-Based Radar System. Primary emphasis is on Van Allen type trapped radiation effects on solar cells and on the antenna transmitter/receiver modules. Qualitative references to man-made nuclear radiation effects are also given. It is concluded that weight penalties for shielding against trapped radiation effects are sufficiently high in the intermediate altitude regime, 2,000 to 9,000 km altitude, to drive the design choices to higher or to lower altitude regimes.

DD FORM 1473 EDITION OF 1 NOV 65 IS OBSOLETE
1 JAN 73

207650